

On the detection of the radiation amplitude zero in $e^\pm p$ collisions

Jim Reid

Department of Physics, University of Tulsa, Tulsa, Oklahoma 74104

G. Li and Mark A. Samuel

Department of Physics, Oklahoma State University, Stillwater, Oklahoma 74078

(Received 19 October 1989)

The processes $e^\pm p \rightarrow e^\pm p \gamma$ are reconsidered. It is shown that the radiation amplitude zero in $e^+ p \rightarrow e^+ p \gamma$ is clearly visible, allowing a direct measurement of the u -quark charge, via real photons. In the case of $e^- p \rightarrow e^- p \gamma$, however, the zero is washed out. These conclusions agree with those of a recent paper by Couture.

A few years ago it was discovered¹ by Mikaelian, Samuel, and Sahdev that the angular distribution for $d\bar{u} \rightarrow W^- \gamma$ ($u\bar{d} \rightarrow W^+ \gamma$) vanishes at a certain angle provided the magnetic moment of the W^\pm has the gauge-theory value $\kappa_W = 1$. They proposed using this peculiar behavior in $p\bar{p}$ and pp collisions, $p\bar{p}$ or $pp \rightarrow W^\pm \gamma X$, where a dip persists, as a means of measuring the magnetic moment of the W . Subsequently, it was shown² that these radiation amplitude zeros are due to the complete destructive interference of the radiation patterns and occur whenever the process contains one real photon, only like-sign charges, and $g=2$ for all particles with spin.

In this Brief Report we discuss the case of the reactions $e^\pm p \rightarrow e^\pm p \gamma$ and demonstrate here how the amplitude zero may be detected.

The underlying parton processes are

$$e^+(p) + u(q) \rightarrow e^+(p') + u(q') + \gamma(k), \quad (1)$$

$$e^+(p) + d(q) \rightarrow e^+(p') + d(q') + \gamma(k), \quad (2)$$

$$e^-(p) + u(q) \rightarrow e^-(p') + u(q') + \gamma(k), \quad (3)$$

and

$$e^-(p) + d(q) \rightarrow e^-(p') + d(q') + \gamma(k), \quad (4)$$

where (1) and (4) contain the amplitude zero (like-sign charges) and (2) and (3) do not. The generalized Mandelstam invariants are

$$\begin{aligned} s &= (p+q)^2, \quad s' = (p'+q')^2, \\ t &= (p-p')^2, \quad t' = (q-q')^2, \\ u &= (p-q')^2, \quad u' = (p'-q)^2. \end{aligned} \quad (5)$$

The electric charges are Q_j for the leptons and Q_i for the quarks $q_i = u$ or d . The photon is radiated off each of the external lines giving four Feynman diagrams. The partial differential cross section^{3,4} may be written as

$$\sigma_0^{-1} \frac{d\sigma}{dx_i dx_j d \cos\theta_\gamma d\phi} = \left[\frac{s^2 + s'^2 + u^2 + u'^2}{tt'} \right] M \left[\frac{s}{4} \right] \quad (6)$$

with

$$\begin{aligned} M = -\frac{\alpha}{8\pi^2} & \left[\frac{Q_i^2 t}{(p \cdot k)(p' \cdot k)} + \frac{Q_j^2 t'}{(q \cdot k)(q' \cdot k)} \right. \\ & + Q_i Q_j \left[\frac{u}{(p \cdot k)(q' \cdot k)} + \frac{u'}{(p' \cdot k)(q \cdot k)} \right. \\ & \quad \left. + \frac{s}{(p \cdot k)(q \cdot k)} \right. \\ & \quad \left. \left. + \frac{s'}{(p' \cdot k)(q' \cdot k)} \right] \right] Q_i^2 Q_j^2 \quad (7) \end{aligned}$$

and

$$\sigma_0 = \frac{\pi\alpha^2}{2s}. \quad (8)$$

The scaled energies of the final-state particles in the (e^\pm, q_j, γ) c.m. frame are x_i, x_j , and x_γ , where $x_i = 2p'_{c.m.} / \sqrt{s}$, etc. Their angles relative to the incident lepton momentum p are θ_i, θ_j , and $\pi - \theta_\gamma$. θ_γ is the angle between the photon momentum and the incident quark momentum. The angle ϕ is that between the plane of the final-state particles in the c.m. frame and the plane of the incident particles and the photon.

The condition for the null zone is given by²

$$\frac{Q_i}{p \cdot k} = \frac{Q_i}{p' \cdot k} = \frac{Q_j}{q \cdot k} = \frac{Q_j}{q' \cdot k}. \quad (9)$$

In the c.m. frame these reduce to two useful conditions:

$$\cos\theta_\gamma = -(Q_i - Q_j)/(Q_i + Q_j) \quad (10)$$

and

$$(1 - x_j)/(1 - x_i) = Q_i/Q_j. \quad (11)$$

For reaction (1) the amplitude zero occurs at

$$\cos\theta_\gamma = 0.2 \quad (12)$$

and for reaction (4) it occurs at

$$\cos\theta_\gamma = 0.5. \quad (13)$$

We note that the parton processes (1)–(4) have also been considered by Bilchak.⁵ In particular, she looks at these reactions as a measure of the quark charges, i.e., how to distinguish fractionally charged quarks from integrally charged quarks. She does not, however, consider the hadronic processes $e^\pm p \rightarrow e^\pm p \gamma$. In this paper we combine the parton cross sections with the proton distribution functions to obtain the hadronic cross sections for $e^\pm p \rightarrow e^\pm p \gamma$.

In order to relate these parton results to actual measur-

able quantities, we first integrate over the final x_i, x_j , and ϕ under the second null-zone constraint equation (11), thus obtaining a partial cross section which is a function of only two variables instead of five: namely, energy, and θ_γ . Then this cross section is convoluted with the proton parton distribution functions in the (e, q, γ) c.m. frame to yield the partial differential cross section for the real physical process $e^\pm p \rightarrow e^\pm p \gamma$. Our result for the hadronic cross section is

$$\frac{d\sigma}{d\cos\theta} = \left(\frac{\pi\alpha^2}{8} \right) f(S\cos\theta) = \int_0^1 dy Pp(y) \int \int \int dx_i dx_j d\phi g(Q_i(1-x_i) - Q_j(1-x_j)) \left(\frac{d\sigma}{dx_i dx_j d\cos\theta d\phi} \right). \quad (14)$$

Here y is the parton momentum fraction, $Pp(y)$ is the parton distribution function, and we have dropped the γ subscript in θ_γ , $\theta_\gamma = \theta$. We have used Eqs. (6)–(8) and the QCD-evolved parton distribution functions of Eichten *et al.*⁶ to obtain the results shown in Figs. 1–7 below.

We choose $x_{i\min} = 0.1$ and $x_{i\max} = 0.9$ throughout this paper. Also, we call $y = x_A$ and use $x_{A\min} = 0.01$ throughout. To be more realistic in comparing with experiment instead of using a δ function $g = \delta$ we use

$$g(x_j - \bar{x}_j) = \begin{cases} N, & \bar{x}_j - R_0 < x_j \leq \bar{x}_j + R_0 \\ 0 & \text{otherwise,} \end{cases} \quad (15)$$

where we normalize g so that

$$N = 1/2R_0 \quad (16)$$

and

$$\bar{x}_j = \begin{cases} (2x_i + 1)/3 & \text{for } Q_j = +1 (e^+ p), \\ (x_i + 2)/3 & \text{for } Q_j = -1 (e^- p). \end{cases} \quad (17)$$

$2R_0$ is the size of the experimental bin around the zero conditions given in Eq. (17) [see Eq. (11)].

Figures 1–3 show our results for $e^+ p (Q_j = +1)$. In Fig. 1 we use

$$R_0 = 2(1 - \bar{x}_j)/5 \quad (18)$$

and we see a significant dip at $\cos\theta = 0.2$ in agreement with Eq. (12). As we decrease the bin size R_0 in Figs. 2 and 3 the dip becomes sharper. In Fig. 2 we use

$$R_0 = (1 - \bar{x}_j)/4 \quad (19)$$

and the dip is quite sharp. In Fig. 3 we use

$$R_0 = (1 - \bar{x}_j)/7. \quad (20)$$

Here the *dip* is very sharp and quite dramatic.

The situation for $e^- p (Q_j = -1)$ is quite different. This can be seen in Figs. 4–7. The bin size is, respectively,

$$R_0 = 2(1 - \bar{x}_j)/5, \quad (21)$$

$$R_0 = (1 - \bar{x}_j)/4, \quad (22)$$

$$R_0 = (1 - \bar{x}_j)/7, \quad (23)$$

$$R_0 = (1 - \bar{x}_j)/13. \quad (24)$$

There is no sign of a dip at $\cos\theta = 0.5$ where it should be according to Eq. (13). The zeros here have been completely washed out. In each case there are two terms contributing to the cross section [see Eqs. (1) and (2) for $Q_j = +1$ and Eqs. (3) and (4) for $Q_j = -1$]. Only one of the two terms in each case has like-sign charges and, hence, a radiation amplitude zero. Nevertheless, in the case of $e^+ p$ there remains a substantial dip. However, in the case of $e^- p$ the zero is completely washed out. In each case we have used $S = (314 \text{ GeV})^2$, 314 GeV being the c.m. energy of DESY HERA (30-GeV electrons on 820-GeV protons). However, the results for other energies

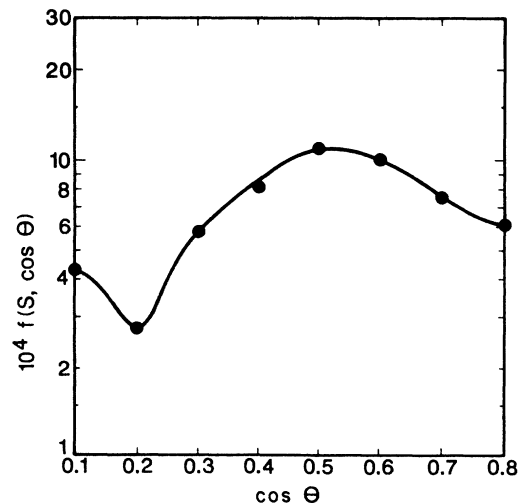


FIG. 1. $f(S, \cos\theta)$ in GeV^{-2} vs $\cos\theta$ for $e^+ p \rightarrow e^+ p \gamma$. $x_{A\min} = 0.01$, $\sqrt{S} = 314 \text{ GeV}$, $\bar{x}_j = (2x_i + 1)/3$, and $R_0 = 2(1 - \bar{x}_j)/5$.

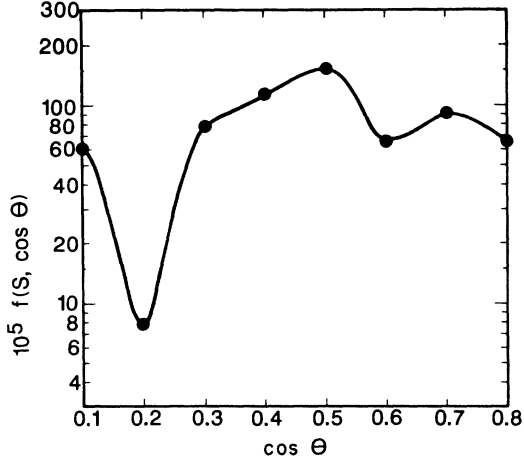


FIG. 2. $f(S, \cos\theta)$ in GeV^{-2} vs $\cos\theta$ for $e^+p \rightarrow e^+p\gamma$. $x_{A \min}=0.01$, $\sqrt{S}=314$ GeV, $\bar{x}_j=(2x_i+1)/3$, and $R_0=(1-\bar{x}_j)/4$.

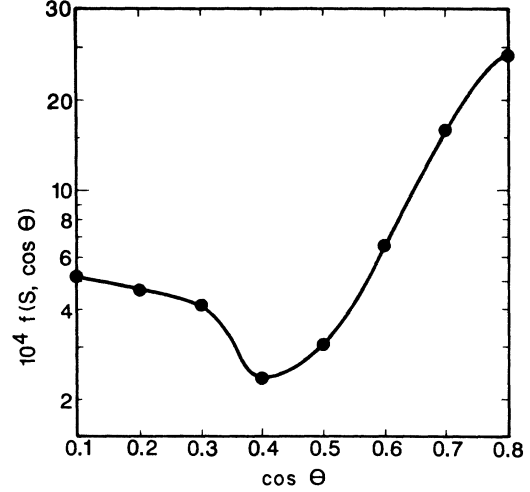


FIG. 4. $f(S, \cos\theta)$ in GeV^{-2} vs $\cos\theta$ for $e^-p \rightarrow e^-p\gamma$. $x_{A \min}=0.01$, $\sqrt{S}=314$ GeV, $\bar{x}_j=(2+x_i)/3$, and $R_0=2(1-\bar{x}_j)/5$.

can be approximately obtained by simply scaling the cross section by $1/S$. For example, from Fig. 3 for $Q_j=+1(e^+p \rightarrow e^+p\gamma)$, $x_{A \min}=0.01$ and $\cos\theta=0.6$ we have $f \sim 8 \times 10^{-5} \text{ GeV}^{-2}$. Thus at $S=(314 \text{ GeV})^2$,

$$\frac{d\sigma}{d\cos\theta} = 1 \text{ pb} \quad (25)$$

and using a luminosity $\mathcal{L}=10^{32} \text{ cm}^{-2}\text{s}^{-1}$ and an experimental time $T=10^7$ s, we obtain approximately 1000 events. This should be a sufficient number. Our cuts should be realistic experimental cuts. Thus when these cuts are made on the data with sufficient counts the dips for e^+p should be clearly visible. Such an experiment could be done at HERA. The position of the dip pro-

vides, according to Eq. (10), a measure of the quark charges via real photons.

We conclude with a note of caution together with a constructive suggestion. The theoretical cross sections which we have presented are calculated in the $(e^\pm q_j, \gamma)$ c.m. frame which is not in general the same as the $(e^\pm p)$ c.m. frame. Cross sections calculated in the $(e^\pm p)$ c.m. frame will exhibit smearing of the different null zones belonging to different parton momenta y , and may not exhibit a dip. How can a cross section of the kind that we have presented be assembled from the experimental events, since the momentum of individual partons is not measurable and is integrated over?

An approximate solution to this problem may be obtained by observing that in the parton integration, the

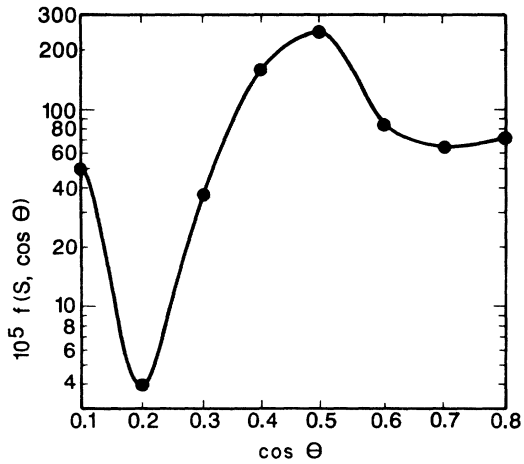


FIG. 3. $f(S, \cos\theta)$ in GeV^{-2} vs $\cos\theta$ for $e^+p \rightarrow e^+p\gamma$. $x_{A \min}=0.01$, $\sqrt{S}=314$ GeV, $\bar{x}_j=(2x_i+1)/3$, and $R_0=(1-\bar{x}_j)/7$.

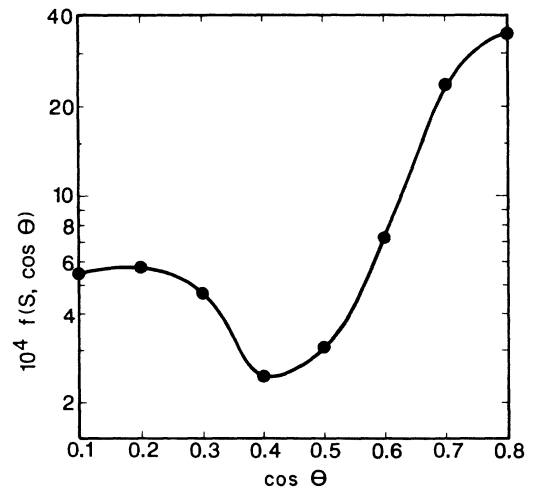


FIG. 5. $f(S, \cos\theta)$ in GeV^{-2} vs $\cos\theta$ for $e^-p \rightarrow e^-p\gamma$. $x_{A \min}=0.01$, $\sqrt{S}=314$ GeV, $\bar{x}_j=(2+x_i)/3$, and $R_0=(1-\bar{x}_j)/4$.

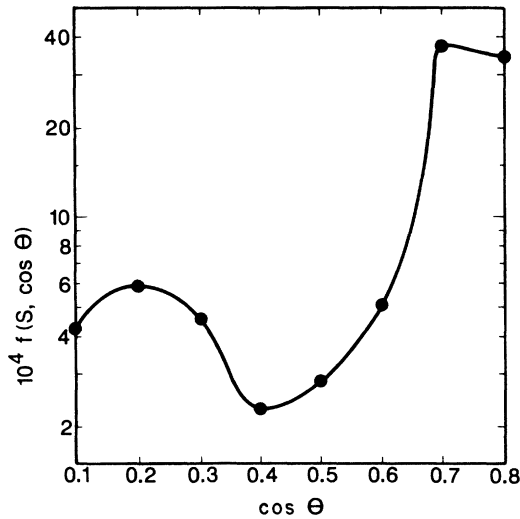


FIG. 6. $f(S, \cos\theta)$ in GeV^{-2} vs $\cos\theta$ for $e^-p \rightarrow e^-p\gamma$. $x_{A \min}=0.01$, $\sqrt{S}=314$ GeV, $\bar{x}_j=(2+x_i)/3$, and $R_0=(1-\bar{x}_j)/7$.

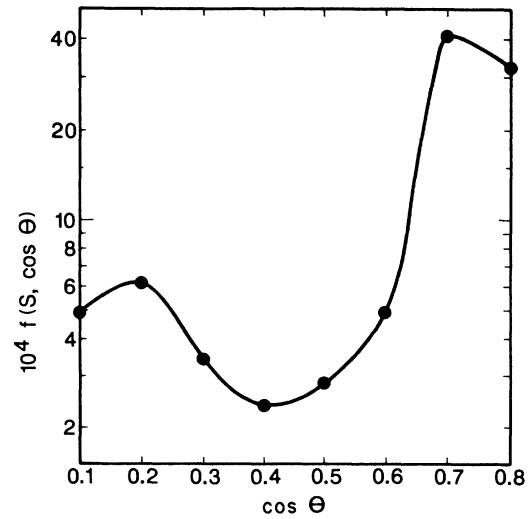


FIG. 7. $f(S, \cos\theta)$ in GeV^{-2} vs $\cos\theta$ for $e^- \rightarrow e^- p\gamma$. $x_{A \min}=0.01$, $\sqrt{S}=314$ GeV, $\bar{x}_j=(2+x_i)/3$, and $R_0=(1-\bar{x}_j)/13$.

bulk of the integral comes from a very restricted region in the vicinity of $y=0$ (roughly $0 \leq y \leq 0.2$). This is because the parton distribution function diverges at $y=0$. The mean value of y is typically $\bar{y} \approx 0.1$. We propose that such a mean value be taken as the basis for the choice of the $(e^\pm q_j \gamma)$ c.m. frame. Once a specific choice is made for y , then all momenta in the problem are fixed by knowledge of the experimentally measurable four-momenta. Each event can be reconstructed and boosted to the c.m. frame, to construct a cross section of the kinds that we have calculated. In this way one might have an experimental cross section to which our results could be compared. The radiation amplitude dip should be very clearly visible in the case $e^+p \rightarrow e^+p\gamma$.

This paper should replace an earlier one⁷ in which Eqs.

(6), (7), and (14) were incorrect. In that paper we also used the less realistic δ function

$$g(x) = \delta(x). \quad (26)$$

Recently we were made aware of a paper by Couture⁸ on this subject. Although his method of binning is slightly different than ours, our results and conclusions agree.

One of us (M.A.S.) would like to thank Gilles Couture for pointing out our errors and very helpful discussions, as well as the Aspen Center for Physics for its kind hospitality. This work was supported by the U.S. Department of Energy under Grant No. DE-FG05-85ER40215.

¹K. Mikaelian, M. A. Samuel, and D. Sahdev, Phys. Rev. Lett. **43**, 746 (1979).

²S. J. Brodsky and R. W. Brown, Phys. Rev. Lett. **49**, 966 (1982); R. W. Brown, K. Kowalski, and S. J. Brodsky, Phys. Rev. D **28**, 624 (1983); M. A. Samuel, *ibid.* **27**, 2724 (1983).

³K. Hagiwara, F. Halzen, and F. Herzog, Phys. Lett. **135B**, 324 (1984).

⁴F. A. Berends, R. Kleiss, P. De Causmaecker, and R. Gastmans, Phys. Lett. **103B**, 124 (1981).

⁵C. L. Bilchak, J. Phys. G **11**, 1117 (1985).

⁶E. Eichten, J. Hinchcliffe, K. Lane, and C. Quigg, Rev. Mod. Phys. **56**, 579 (1984).

⁷Mark A. Samuel and Jim Reid, Phys. Rev. D **35**, 3505 (1987).

⁸Gilles Couture, Phys. Rev. D **39**, 2527 (1987).